A Comparative Autoradiographic Study Demonstrating Differential Intratumor Localization of Monoclonal Antibodies to Cell Surface (Lym-1) and Intracellular (TNT-1) Antigens

Feng-Ming Chen, Alan L. Epstein, Zhen Li, and Clive R. Taylor

Department of Pathology, University of Southern California, Los Angeles, California

Autoradiography was utilized to explore the patterns of distribution of two different monoclonal antibodies (Lym-1 and TNT-1) in tumor-bearing nude mice. Lym-1 is an antibody against a cell surface B-cell antigen. In comparison, TNT-1 represents a novel approach and is an antibody against an intracellular (nuclear) antigen that is selectively revealed in degenerating tumor cells. Experimentally iodine-125-(^{125}I) labeled Lym-1 or TNT-1 was injected intravenously into nude mice bearing either the Raji lymphoma or the ME-180 human cervical carcinoma. Qualitative autoradiographic analyses performed after injection revealed that Lym-1 accumulated at the periphery of the target tumor where vascular permeability is marked and where Lym-1-positive cells are first encountered. By contrast, TNT-1 lost its initial peripheral distribution and demonstrated progressive concentration in the center of the tumor where binding to its nuclear antigen is facilitated by the presence of cell degeneration and necrosis. These studies confirm the ability of TNT-1 to bind areas deep within tumor that traditionally are considered inaccessible to antibodies administered for imaging and therapy.

J Nucl Med 1990; 31:1059–1066

The effectiveness of monoclonal antibodies in the treatment of cancer is dependent not only upon the specificity of the antibody for antigen present in the tumor, but also upon the distribution and accessibility of antigen throughout the lesion, and the effectiveness of delivery of immunologically active antibody to the tumor site.

The issue of "tumor-associated antigens," their existence or otherwise, has been much debated, along with problems resulting from the heterogeneity of antigen expression within individual tumors and antigen modulation that may be induced by recurrent encounters with antibody (*1–5*). In tacit recognition of the problems inherent in developing monoclonal antibodies that are tumor-specific, imaging and therapy trials have commenced using antibodies that are "relatively" tumor-specific, in that the target antigens, while richly expressed on malignant cells, are not entirely restricted to tumor tissue. The use of monoclonal antibodies B72.3 (*6*), Lym-1 (*7, 8*), and anti-CEA monoclonal antibodies (*9*), represent examples of this approach.

In previously reported studies (*10,11*), we have adopted a novel method that does not rely upon the selective specificity of antibody for malignant cells, but rather exploits a unique aspect of the pathophysiology of the neoplastic population, namely the characteristic presence of a high proportion of degenerating cells within the tumor. The abnormal membrane permeability displayed by these degenerating tumor cells makes the cell interior accessible, allowing circulating antibody to bind to the nuclear antigens. It is this characteristic that differentiates the tumor from normal tissues, facilitating the preferential accumulation of an anti-nuclear antibody in a wide variety of human cancers.

With this approach, successful imaging and treatment of a variety of transplantable tumors in a nude mice model have been achieved by targeting nuclear antigens revealed in necrotic tumors using an antibody (TNT-1) against nuclear histones (*10, 11*). Designated TNT (tumor necrosis treatment), this approach provides the opportunity to study factors affecting antibody delivery to the tumor site, as well as diffusion and localization of antibody within the substance of the tumor. As described previously by other laboratories (*12–14*), autoradiographic techniques allow the qualitative analysis of the pattern of diffusion of labeled antibody within

Received Oct. 3, 1989; revision accepted Dec. 26, 1989.

For reprints contact: Clive R. Taylor, MD, PhD, Professor and Chairman, Department of Pathology, University of Southern California, 2011 Zonal Ave.-HMR 204, Los Angeles, CA 90033.

tumors, the sites of antibody localization, and the retention of antibody over several days in the face of progressive clearance of antibody from the blood pool.

In order to analyze the pattern of distribution of TNT-1 antibody with reference to more conventional antibody imaging and therapy techniques, parallel studies were performed using a second antibody (Lym-1) directed at the cell surface of lymphomas in tumor-bearing nude mice. The results of these experiments lend further support to the contention that TNT is a promising new approach for the imaging and treatment of cancer.

MATERIALS AND METHODS

Monoclonal Antibodies

The production, purification, and characterization of monoclonal antibody TNT-1 (IgG2a) have been previously described (*10, 11*).

Lym-1 (IgG2a), a monoclonal antibody reactive with the cell surface of B-lymphocytes (*15*), was obtained from Techniclone International, Inc. (Tustin, CA). Iodine-131 radiolabeled Lym-1 has been shown to give successful imaging and therapy in transplantable lymphomas as well as lymphoma patients in Phase I clinical trials (*7, 8*). SDS-polyacrylamide gel electrophoresis demonstrated that both antibodies were >95% pure. Protein concentrations of the antibody preparations were estimated by optical spectroscopy at 280 nm.

Radioiodination and Immunoreactivity of Antibodies

TNT-1 and Lym-1 monoclonal antibodies were radiolabeled with ^{125}I (New England Nuclear Co., Boston, MA) by the chloramine-T method (*16*). Briefly, the iodination reaction was initiated by adding chloramine-T (Sigma Chemical Co., St. Louis, MO) at a weight ratio of 10:1 (antibody:chloramine-T). After terminating the reaction by the addition of sodium metabisulfite (Mallinckrodt, Inc., St. Louis, MO), the reaction mixture was chromatographed on a Sephadex G-25 (Sigma Chemical Co., St. Louis, MO) gel column that was previously equilibrated with phosphate-buffered saline (PBS) containing 1% bovine serum albumin (Sigma Chemical Co., St. Louis, MO). Fractions of ^{125}I-labeled monoclonal antibodies were collected and then diluted with PBS to an appropriate volume for injection.

Immunoreactivities for each radiolabeled antibody preparation were monitored by radioimmunoassay. Approximately 75%-80% of radiolabeled Lym-1 preparations were found to bind Raji cells by live cell radioimmunoassay as previously reported (*15*).

The radiolabeled TNT-1 showed >80% of immunoreactivity in a paraformaldehyde-acetone-treated cell assay developed in our laboratory (*17*). Briefly, the radiolabeled TNT-1 was incubated for 30 min with Raji cells which were previously fixed with 10% paraformaldehyde and then treated with −20°C acetone. The cells were then washed with PBS (3×) and counted in a gamma counter (LKB, 1282 compugamma CS model, Pleasant Hill, CA).

Tumor Model and Experimental Design

Six-week-old female athymic nude mice (Charles River, Wilmington, MA) were injected subcutaneously in the thigh with 10^7 ME-180 tumor cells in 0.2 ml RPMI 1640 medium (Gibco Laboratories, Grand Island, NY) containing 10% fetal calf serum (Hyclone Laboratories, Logan, UT), 100 units/ml Penicillin G, and 100 μg/ml streptomycin sulfate. Animals were utilized for studies when the tumors measured ~1 cm in maximal diameter. Raji lymphomas were grown in nude mice by similar techniques (*15*).

Radioiodinated antibodies were injected into groups of nude mice bearing either the ME-180 human cervical carcinoma or the Raji lymphoma as follows: Group A (n = 7), mice with ME-180 tumors received ^{125}I-TNT-1; Group B (n = 7), mice with ME-180 tumors received ^{125}I-Lym-1; Group C (n = 7), mice with Raji tumors received ^{125}I-Lym-1; and Group D (n = 7), mice with Raji tumors received ^{125}I-TNT-1. A dose of 60 μCi/50 μg per mouse of the ^{125}I-labeled antibodies was administered intravenously via the lateral tail vein. Following the injections, one mouse from each group was killed at 1 hr, 6 hr, 1 day, 2 days, 3 days, 5 days, and 7 days. The tumor implants and selected normal tissues (liver, kidney) were excised, fixed overnight in 10% buffered formalin, and paraffin embedded. Sections (5 μm) of the embedded tissues were mounted on acid-cleaned glass slides and deparaffinized with xylene. The slides were either stained with Hematoxylin and Eosin (H&E), or used for autoradiographic studies as described below.

Autoradiography

Macroautoradiography was performed by placing slides bearing tissue sections in direct contact with single-coated x-ray film (SB-5; Kodak, Rochester, NY) in x-ray cassettes, and exposed 3–14 days at room temperature. Exposed films were developed in an automatic developer (Kodak M35A X-OMAT Processor) and air dried.

For micro-autoradiography, Ilford K5D nuclear emulsion (Polyscience, Inc., Warrington, PA) was melted in a coplin jar in a water bath at 45°C, stirring gently to avoid local overheating. The emulsion was used without dilution and care was taken not to agitate to a degree that produced foam. Slides were then dipped in the emulsion, air dried in a vertical position, and stored in a light-proof box for 3–12 days before developing in Dektol (Kodak, Rochester, NY) for 2 min. They were then fixed and counterstained with H&E, dried, and mounted for microscopic examination. The specific location and the distribution of the radiolabeled monoclonal antibody in the tissues was revealed by the distribution of silver grains.

RESULTS

Macroautoradiographic Studies

Tumor, together with normal liver and normal kidney, was sampled at intervals following injection of standardized doses of labeled antibody as described above. In each instance, the tumor was bisected across its maximum girth, and sections were employed both for macroautoradiography and for the preparation of microscopic slides coated with photographic emulsion.

The findings in the macroautoradiographs are illustrated in Figures 1–6. Lym-1 injected into mice bearing Raji tumors showed progressive concentration of label at the tumor periphery from 1 hr (Fig. 1), to 6 hr, to 24 hr. At 3, 5, and 7 days postinjection, the peripheral

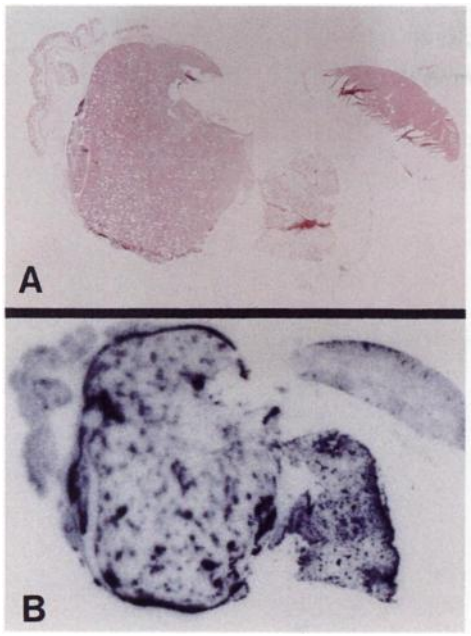

FIGURE 1
Raji lymphoma and normal tissues (lung and liver) showing (A) H&E appearance and (B) macroautoradiography 1 day after the i.v. injection of ^{125}I-Lym-1. Label is concentrated at the tumor periphery, with focal condensations centrally in relation to blood vessels. The blood pool has not yet cleared and normal tissues show labeling due to their blood content.

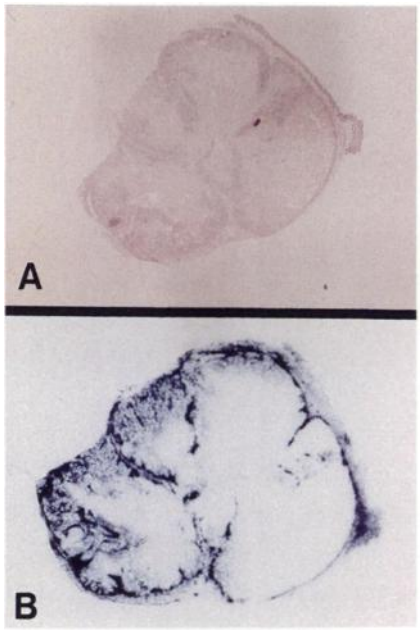

FIGURE 3
ME-180 cervical carcinoma showing (A) H&E appearances and (B) macroautoradiography 1 hr after i.v. injection of ^{125}I-TNT-1. Labeling is restricted to the zone of richly perfused permeable vessels at the tumor periphery. The H&E section reveals extensive degeneration and necrosis in this tumor, and also in the tumors depicted in Figures 4–6.

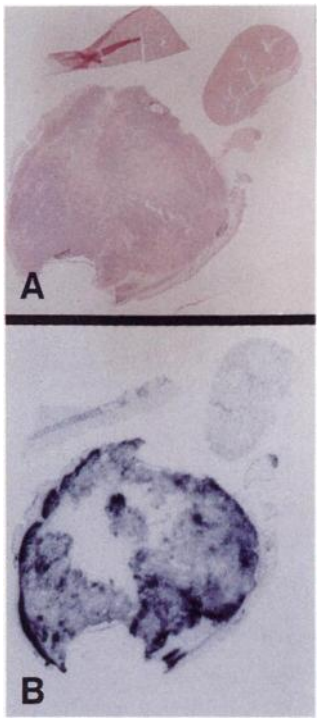

FIGURE 2
Raji lymphoma and normal tissues (kidney, liver) showing (A) H&E appearances and (B) macroautoradiography 7 days after i.v. injection of ^{125}I-Lym-1. Label remains localized peripherally and in a perivascular location bound to tumor cells. The blood pool has cleared of the antibody and normal tissues show no evidence of label.

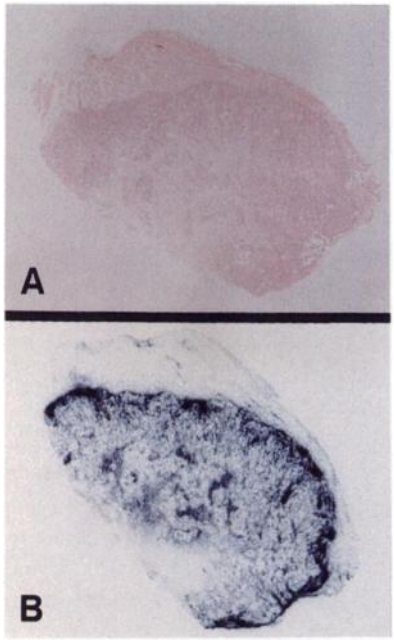

FIGURE 4
ME-180 cervical carcinoma showing (A) H&E appearances and (B) macroautoradiography 6 hr after i.v. injection of ^{125}I-TNT-1. Labeling of the periphery still is apparent, but diffusion of label into the tumor substance already is seen.

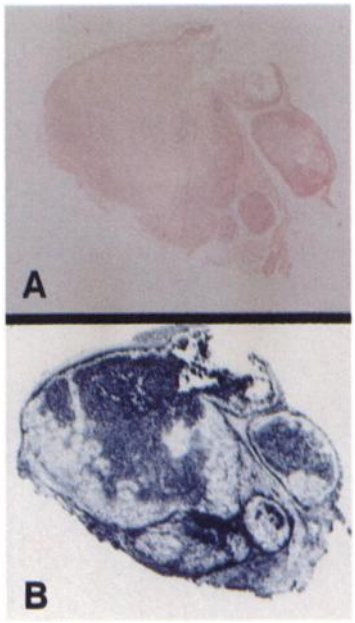

FIGURE 5
ME-180 cervical carcinoma showing (A) H&E appearances and (B) macroautoradiography 2 days after i.v. injection of ^{125}I-TNT-1. Degenerating and necrotic regions deep within the tumor show heavy labeling.

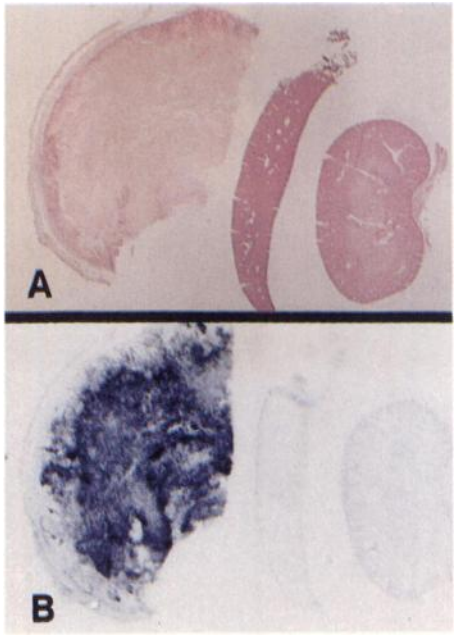

FIGURE 6
ME-180 cervical carcinoma and selected normal tissues (liver and kidney) showing (A) H&E appearances and (B) macroautoradiography 7 days after i.v. injection of ^{125}I-TNT-1. There is now little residual labeling of the peripheral parts of the tumor, but dense deposits are present in the deep regions corresponding to areas of degeneration and necrosis. Normal tissues show complete clearance of the labeled TNT-1.

localization was maintained or intensified in all cases. Some foci of labeling became apparent deep within the tumor at 2 days and persisted through 7 days (Fig. 2). At microscopic examination, these foci were seen to occur in relation to vessels penetrating the tumor core.

TNT-1 injected into mice bearing ME-180 carcinoma showed a rather different distribution. At 1 hr, there was dense labeling of the tumor periphery (Fig. 3). At 6 hr (Fig. 4) and 24 hr, peripheral concentration was still apparent, but an increasing amount of label was seen deep within the tumor, not restricted to a perivascular location. At 2 days, the intensity of labeling in the central region matched or exceeded that of the periphery (Fig. 5). Subsequently, as the periphery showed partial clearance, the intensity of labeling in the tumor core continued to increase from 3–7 days (Fig. 6).

Lym-1 injected into mice bearing the ME-180 carcinoma showed an early phase of peripheral localization at 1 and 6 hr that then faded rapidly (24 hr) and was no longer apparent in tumor sampled on Days 3, 5, or 7. There was no appreciable labeling of the tumor core.

TNT-1 injected into mice bearing the Raji lymphoma also showed a phase of peripheral localization at 1 and 6 hr. The intensity of labeling, however, was never as great as that achieved by the corresponding dose of Lym-1 in Raji tumors. Subsequently, peripheral labeling attributable to TNT-1 faded rapidly and was succeeded by patchy labeling of the deeper parts of the tumor at 2, 3, and 5 days. The intensity of labeling by TNT-1 within the deeper parts of the Raji lymphoma was considerably less than for TNT-1 in the ME-180 tumor, showing a broad correlation with the presence and extent of tumor cell degeneration, which was patchy in Raji lymphomas but extensive and confluent in the central regions of ME-180 carcinomas.

Microscopic Autoradiographic Studies

Autoradiographic studies at the microscopic level confirmed the distributions reported above, while adding a more detailed picture of localization at the cellular level.

For both Lym-1 and TNT-1, the initial phases of peripheral localization in Raji and ME-180 tumors were largely accounted for by the presence of label confined to the vascular pool within richly anastomosing networks of small vessels at the tumor periphery (Fig. 7A). At 1 hr, most of the label was seen within vessels or in the immediate perivascular extracellular fluid (ECF) (Fig. 7B). At 6 and 24 hr, an increasing amount of label was seen in the ECF, while the density of label within the vascular lumen decreased progressively. At 2 days or beyond, little label was seen within blood vessels.

Microscopic examination of sections from the Lym-1 Raji model showed that while the density of label in the ECF increased progressively from 1 hr to 3 days, label remained localized to tumor cells in the perivascular area and relatively little label was seen in the deeper parts of the tumor, except where rare vessels penetrated to the tumor core.

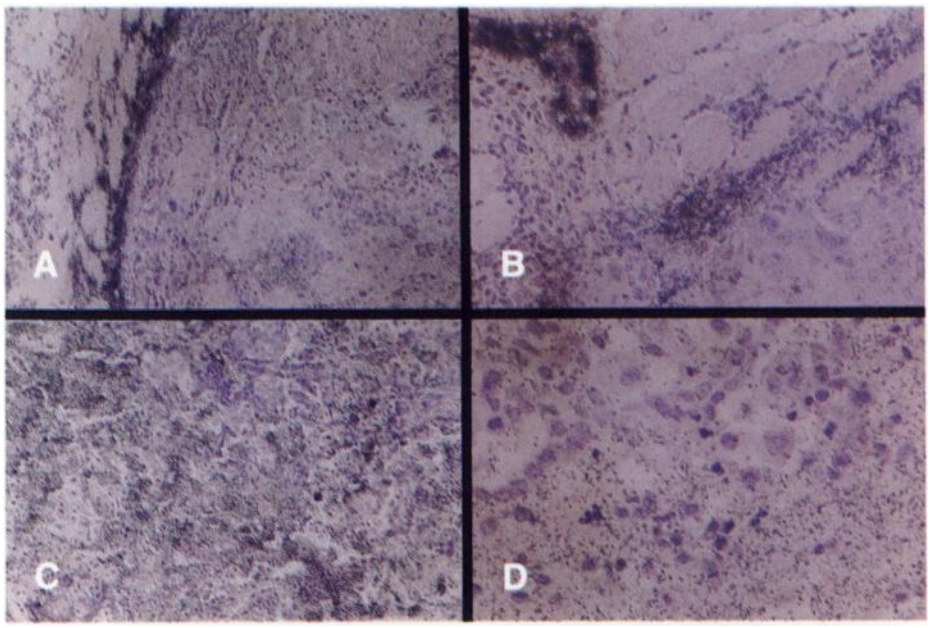

FIGURE 7
(A) Microscopic autoradiograph of ME-180 cervical carcinoma examined 1 hr after i.v. injection of ^{125}I-TNT-1. Labeled antibody is concentrated at the tumor periphery in a region characterized by a rich network of abnormally permeable vessels. Label present in deeper parts of the tumor is related to overall vessels penetrating this region. (H&E, silver emulsion autoradiograph: original magnification, ×25). (B) Microscopic autoradiograph of ME-180 cervical carcinoma examined 1 hr after i.v. injection of ^{125}I-TNT-1. Detailed examination shows that much of the labeled antibody is still within the vascular pool, but that diffusion into the tumor ECF has begun. (H&E, silver emulsion autoradiograph: original magnification, ×100). (C) Microscopic autoradiograph of ME-180 cervical carcinoma examined 2 days after i.v. injection of ^{125}I-TNT-1. Dense deposits of silver grains are seen overlying areas of tumor cell degeneration and necrosis. (H&E, silver emulsion autoradiograph: original magnification, ×250). (D) Microscopic autoradiograph of ME-180 cervical carcinoma examined 7 days after i.v. injection of ^{125}I TNT-1. Silver grains are present in areas of amorphous necrosis. While some labeled tumor cells show evidence of degeneration, many do not. The presence of labeled antibody in these cells is indicative of abnormally permeable cell surface membrane in vivo. (H&E, silver emulsion autoradiograph: original magnification, ×400).

In contrast, label extended beyond the perivascular ECF in the TNT-1 treated ME-180 tumors at 1 and 6 hr, was already detectable in deeper regions of the tumor at 24 hr, and increased in concentration at 2 days. Microscopically, label was present diffusely in areas of amorphous necrosis (Fig. 7C) but was also concentrated in tumor cells bordering these necrotic areas (Fig. 7D). In some instances, labeled cells showed evidence of cellular degeneration, such as karyorrhexis or karyolysis, but other labeled cells displayed none of the cytologic stigmata of cell degeneration or necrosis, as shown in Fig. 7D.

Examination of Raji tumors from TNT-1-injected animals revealed some parallels with the TNT-ME-180 model, except that overt necrosis was much less evident in Raji lymphomas compared with ME-180 tumors. Distribution of labeled TNT-1 in Raji tumors was thus restricted to patchy areas deep within the tumor. Analogous with the ME-180 model, only some of these tumor cells showed morphologic criteria of cell degeneration evidenced by orthodox light microscopy.

DISCUSSION

The goal of this study was to examine the importance of antigen distribution and accessibility in determining the localization of monoclonal antibody in tumors in vivo. For this purpose, we used two monoclonal antibodies, both of IgG2a subclass, but with differing specificity characteristics. One, designated Lym-1, reacts with a surface antigen present on lymphoma cells and has been used successfully to image and treat human B-cell lymphomas in animal models and in man (*7*, *8*). The other, designated TNT-1, reacts with an intracellular antigen that is rendered accessible to injected antibody by changes in cell membrane permeability occurring as a consequence of cellular degeneration or necrosis within tumors. TNT-1 has successfully demonstrated imaging and therapy of several histologic types of human solid tumors in animal models (*10*, *11*), and a trial of its capability for imaging tumors in man has commenced.

The conventional approach to the use of monoclonal antibodies in imaging or therapy of tumors employs antibody with specificity for an antigen present on the surface of tumor cells (*3*, *4*), here represented by Lym-1. Disadvantages of this approach include antigen modulation, heterogeneity of expression of antigen by tumor cells, and problems inherent in developing antibodies that are tumor specific (*1*, *5*). In addition, our autoradiographic studies with ^{125}I-Lym-1 in the Raji lym-

phoma model demonstrate that this type of antibody shows preferential concentration at the periphery of tumors or perivascularly, with poor diffusion into the deeper regions (Figs. 1 and 2). These results compare favorably with other autoradiographic studies describing the localization of cell surface specific monoclonal antibodies administered to tumor-bearing nude mice. Studies by Pervez et al. (*13*) and Jones et al. (*12*) clearly demonstrated the perivascular accumulation of antibody at the periphery of tumor. Along with Ong and Mattes (*14*), these studies conclude that unlike highly vascularized viable areas of the tumor, centrally located pockets of cells and necrotic zones appear not to be accessible to antibody penetration.

In contrast to the above approach, TNT circumvents many of these problems and facilitates penetration of antibody into the core of the tumor. In this instance, a monoclonal antibody (TNT-1) is directed against a histone antigen in the cell nucleus, and is totally devoid of reactivity to cell surface antigens. TNT-1 therefore will not bind to the surface of any cell, normal or neoplastic, but is potentially able to bind to the nuclei of all cells. Differential concentration of TNT-1 in tumor is a result of the presence within malignant tumors of numerous degenerating or necrotic cells, all of which possess abnormally permeable cell surface membranes, and the dearth of such cells in normal tissues.

When injected intravenously into either the Raji or ME-180 tumor models, both Lym-1 and TNT-1 show an initial localization at the tumor periphery (compare Figs. 1 and 3). In the earlier stages, label is seen primarily within the blood vessels (i.e., still within the blood pool), with some entry of label into the tumor extracellular fluid, usually in the proximity of vessels recognizable in the plane of the section by microscopic autoradiography (Fig. 7B). Normal tissues (lungs, liver, kidney), examined simultaneously, also showed the presence of label within an hour of injection, but this was almost entirely confined to the vascular pool. Leakage of label into the extracellular fluid was not seen in normal tissues even in later stages of the study. Thus, initial localization of label was primarily determined by blood flow in the rich vascular network at the tumor periphery, and by the excessive permeability of these vessels allowing rapid escape of antibody into the perivascular ECF (*18*).

At 6 and 24 hr, both Lym-1 and TNT-1 still showed a predominance of label at the tumor periphery (Fig. 4), but microscopic examination now showed that an increasing proportion of the label was extravascular. At this stage, differences in distribution for Lym-1 in the Raji lymphoma and TNT-1 in the ME-180 carcinoma, first became apparent and was progressively more marked with the passage of time. In the TNT-1 ME-180 model, label was also detectable in deeper parts of the tumor, within the tumor extracellular fluid, and even within some tumor cells, although amorphous areas of necrosis identified deep within the tumor showed only light labeling at this stage. From 2 to 7 days the pattern of distribution of label TNT-1 in the ME-180 tumor showed further significant change. Macroautoradiography revealed progressive concentration of label in the deeper parts of the tumor (Figs. 5 and 6). Microscopic autoradiography confirmed the presence of label within areas of amorphous necrosis, with particular concentration in adjacent areas of morphologically intact tumor cells (Fig. 7C-D). In many instances, labeled tumor cells showed cytologic evidence of cellular degeneration or necrosis, such as karyolysis or karyorrhexis. However, in other instances, tumor cells showed aggregates of label, but no microscopic evidence of degeneration (Fig. 7D): these presumably represent cells in early phases of degeneration that show abnormal membrane permeability but do not yet manifest any of the cytologic hallmarks of degeneration which occur only in more advanced stages. The numbers of degenerating cells were greatest in the deeper regions bordering areas of overt necrosis, which tended to be situated distantly from recognizable blood vessels, as is consistent with the earlier observations of Thomlinson and Gray (*19*).

Thus TNT-1 showed the ability to penetrate to the core of the ME-180 tumor over a period of two days, even into areas of overt necrosis. Furthermore, labeling was retained or even intensified over subsequent days, up to the 7th day when the experiment was terminated. It is notable that the concentration of TNT-1 within the tumor clearly occurred in the presence of relatively poor blood flow centrally, as deduced from the presence of ischemic necrosis and the paucity of blood vessels observed in the deeper regions. Concentration of TNT-1 in the tumor, with reference to normal tissues that are well perfused, is attributable not only to its binding to antigen within tumor, but also to the enhanced permeability of tumor blood vessels for immunoglobulins. Thus, although the injected TNT-1 clearly reaches normal tissues in the bloodstream, very little antibody leaves the blood in normal tissues (*20*). By contrast, antibody readily escapes the blood in the vicinity of the tumor due to enhanced permeability of the vascular network (*19–21*). The presence of inflammation may account for some of these permeability changes (*22, 23*). However, vessels within the tumor also show marked structural abnormalities, with incomplete walls, abnormal fenestration of the endothelium, or even partial or complete absence of endothelium, forming broad channels that are lined by bare tumor cells (*24*). In these situations, although blood flow is slow, injected TNT-1 has free access to the tumor extracellular fluid and to the tumor cells themselves.

Another interesting finding derives from comparative

observations of the patterns of TNT-1 distribution in the ME-180 tumor and Lym-1 distribution in the Raji tumor. Both TNT-1 and Lym-1 are IgG2a antibodies, presumably therefore displaying similar diffusion characteristics across endothelium and through extracellular fluid. As noted, both TNT-1 and Lym-1 showed initial concentration at the tumor periphery where perfusion and permeability are high (Figs. 1, 3, and 7A). This observation held true for TNT-1 when injected in the Raji model, as well as in its preferred target, the ME-180 model, and for Lym-1 in the ME-180 model, as well as in its preferred target, the Raji tumor. However, after 6 or more hours, progressive differences in distribution were observed. Whereas TNT-1 in the ME-180 model showed some degree of clearance from the periphery and increasing concentration in deeper regions with the passage of time (Figs. 4, 5, and 6), Lym-1 in the Raji model showed persistence of dense labeling at the tumor periphery (Figs. 1 and 2), and relatively little penetration into the center of the tumor except in a perivascular distribution where vessels were identifiable penetrating the depth of the lesion. Upon reflection, these differences in patterns of labeling appear to be attributable to differences in distribution of the respective antigens within the tumor. Following escape from the permeable vasculature at the tumor periphery, Lym-1 immediately encounters its antigen on the surface of essentially all of the Raji tumor cells and is bound. Diffusion in the ECF away from blood vessels therefore is prevented, until such a time as Lym-1 sites in the immediate vicinity of the blood vessels are saturated, if such ever occurs. By contrast, TNT-1 upon leaving vessels at the tumor periphery encounters nuclear antigen only where there are abnormally permeable tumor cells, and these cells are relatively few in number in well perfused areas. TNT-1 therefore is free to diffuse in the ECF along a concentration gradient into avascular areas that do contain large numbers of degenerating cells. These abnormally permeable cells permit entry of the TNT-1 into the cell interior with binding to nuclear antigen, producing maximum labeling at sites remote from blood vessels.

These assumptions were reinforced by observations of the patterns of distribution of Lym-1 in the ME-180 tumor, which contains no Lym-1-positive cells. In this model, Lym-1 showed an early phase of escape into the ECF at the tumor periphery, followed by more general diffusion into the tumor. However, as Lym-1 cleared from the blood stream, so the concentration gradient reversed, and in the absence of its corresponding antigen, Lym-1 washed from the tumor. Similarly, TNT-1 injected into the Raji tumor showed early concentration at the tumor periphery, paralleling Lym-1, but not encountering antigen (permeable or necrotic cells), TNT-1 then diffused widely, attaining higher concentrations in deeper parts of the tumor, in marked contrast to the pattern observed for Lym-1 in the Raji tumor. The density of labeling of TNT-1 in the Raji tumor was less than that observed for TNT-1 in the ME-180 tumor, a finding that we attribute to the presence of fewer degenerating or necrotic cells in the Raji tumors at this stage of its growth. The Raji tumor, containing as it does fewer abnormally permeable cells, presents fewer nuclei as targets for the localization of the TNT-1 antinuclear antibody. Because of the ability of TNT-1 to penetrate deep within tumors and bind with degenerating cells, it may be especially valuable as an adjuvant following conventional cytoreductive therapy, including the use of other monoclonal antibodies.

SUMMARY

TNT-1 antibody is able to achieve significant penetration of avascular areas of tumors. Escape of the antibody from the blood stream is facilitated by the presence of an abnormally permeable vasculature, due in part to the effects of inflammation and in part to structural defects of vessels in the tumor. Diffusion of TNT-1 antibody in the ECF is favored by a concentration gradient that is maintained by the presence in the tumor core of an "antigen sink" consisting of nuclear antigens exposed by tumor cell degeneration and necrosis. By contrast, monoclonal antibodies (such as Lym-1, B72.3, anti-CEA) used in a more conventional manner and directed against antigen distributed on the surface of tumor cells are likely to remain primarily concentrated in an immediate perivascular location at the site of initial encounter with antigen, thereby prohibiting diffusion to deeper parts of the tumor. TNT-1 lends itself not only to the imaging and treatment of diverse histologic types of tumor (the only requirement is for the presence of degenerating or necrotic cells), but also is particularly suited for use with large avascular and necrotic tumors, where alternative therapies generally are not available.

ACKNOWLEDGMENTS

The investigators wish to thank Mrs. Pat Buckley for assistance in preparation of tissue sections, Mr. Nick Douglas for photographic expertise, Mr. Gordon Miller for technical assistance, and Mrs. Betty Redmon for deciphering and editing the manuscript.

REFERENCES

1. Klein G. Tumor specific transplantation antigens. G.H.A. Clowes Memorial Lecture. *Cancer Res* 1968; 28:625–655.
2. Old LJ. Cancer immunology: the search for specificity. *Cancer Res* 1981; 41:361–375.
3. Reisfeld RA, Greene MI, Yacki A. Monoclonal antibodies—progress in cancer immunobiology and clinical applications. *Cancer Res* 1986; 46:2193–2196.
4. Rosen ST, Winter JN, Epstein AL. Application of monoclonal antibodies to tumor diagnosis and therapy. *Ann Clin Lab Sci* 1983; 13:173–184.

5. Hand PM, Nuti M, Colcher D, Schlom J. Definition of antigenic heterogeneity and modulation among human mammary carcinoma cell populations using monoclonal antibodies to tumor associated antigens. *Cancer Res* 1983; 43:728–735.
6. Colcher D, Esteban JM, Carrasquillo JA, et al. Quantitative analyses of selected radiolabeled monoclonal antibody localization in metastatic lesions of colorectal cancer patients. *Cancer Res* 1987; 47:1185–1189.
7. DeNardo SJ, DeNardo GL, O'Grady LF, et al. Treatment of a patient with B cell lymphoma by I-131 Lym-1 monoclonal antibodies. *Intl J Biol Markers* 1987; 2:49–53.
8. DeNardo SJ, DeNardo GL, O'Grady LF, et al. Pilot studies of radioimmunotherapy of B-cell lymphoma and leukemia using I-131-Lym-1 monoclonal antibody. *Antibody, Immunoconjugates, and Radiopharmaceuticals* 1988; 1:17–33.
9. Mach J-P, Carrel S, Forni M, Ritschard J, Donath A, Alberto P. Tumor localization of radiolabeled antibodies against carcinoembryonic antigen in patients with carcinoma. *N Engl J Med* 1980; 303:5–10.
10. Epstein AL, Chen FM, Taylor CR. A novel method for the detection of necrotic lesions in human cancers. *Cancer Res* 1988; 48:5842–5848.
11. Chen FM, Taylor CR, Epstein AL. Tumor necrosis treatment of ME-180 human cervical carcinoma model with ^{131}I labeled TNT-1 monoclonal antibody. *Cancer Res* 1989; 49:4578–4585.
12. Jones PL, Gallagher BM, Sands H. Autoradiographic analysis of monoclonal antibody distribution in human colon and breast tumor Xenografts. *Cancer Immunol Immunother* 1986; 22:139–143.
13. Pervez S, Eppenetos AA, Mooi WJ, et al. Localization of monoclonal antibody AUA1 and its F(ab')$_2$ fragments in human tumour xenografts: An autoradiographic and immunohistochemical study. *Int J Cancer* 1988; (suppl)3:23–29.
14. Ong GL, Mattes MJ. Penetration and binding of antibodies in experimental human solid tumors grown in mice. *Cancer Res* 1989; 49:4264–4273.
15. Epstein AL, Marder RJ, Winter JN, et al. Two new monoclonal antibodies, Lym-1 and Lym-2, reactive with human B lymphocytes and derived tumors, with immunodiagnostic and immunotherapeutic potential. *Cancer Res* 1987; 47:830–840.
16. McFarlene AS. Labelling of plasma proteins with radioactive iodine. *Biochem J* 1956; 62:135–143.
17. Gaffar S, Epstein AL. Cell based radioimmunoassays to quantitate the immunoreactivity of TNT monoclonal antibodies directed against intracellular antigens. *Hybridoma* 1990: in press.
18. Dvorak HF, Nagy JA, Dvorak JT, Dvorak AM. Identification and characterization of the blood vessels of solid tumors that are leaky to circulating macromolecules. *Am J Path* 1988; 133:95–109.
19. Thomlinson RK, Gray LM. The histological structure of some human lung cancers and possible implications for radiotherapy. *Br J Cancer* 1955; 9:539–549.
20. Jain RK. Delivery of novel therapeutic agents in tumors: physiological barriers and strategies. *J Natl Cancer Inst* 1989; 81:570–576.
21. Majno G, Palade GE, Schoefl GI. Studies on inflammation II. The site of action of histamine and serotonin along the vascular tree: a topographic study. *J Biophys Biochem Cytol* 1961; 11:607–626.
22. Fischman AJ, Rubin RH, Khaw BA, et al. Detection of acute inflammation with ^{111}In-labeled nonspecific polyclonal IgG. *Semin Nucl Med* 1988; XVIII:335–344.
23. Morrel EM, Tompkins RG, Fischman AJ, et al. Autoradiographic method for quantitation of radiolabeled proteins in tissues using indium-111. *J Nucl Med* 1989; 30:1538–1545.
24. Warren BA. The vascular morphology of tumors. In: Peterson HI, ed. *Tumor blood circulation*, Orlando, FL: CRC Press: 1979:77–85.

Editorial: One Step Forward with Nonspecifically-Specific Monoclonal Antibodies

Although the monoclonal antibody technology introduced by Kohler and Milstein (*1*) provided initial "great expectations" in the search for the proverbial "magic bullet," it has proven very difficult to develop clinically useful monoclonal antibodies against human tumors for radioimmunoimaging and radioimmunotherapy. The present state-of-the-art requires different antibodies for different tumor types. Recent clinical trials have offered some encouraging results, but inevitably poor tumor localization significantly limits the efficacy of each new monoclonal antibody.

The problems associated with the use of monoclonal antibodies in tumor detection and therapy are well known. Heterogeneity in the distribution of antibodies may result from nonuniform expression of target tumor markers, irregular tumor vasculature, and aberrant microdiffusion dynamics (*2–5*). Nonuniform disposition of malignant cells within the tumor mass, as well as the variable expression of tumor markers on the tumor cells, and the continuous release of tumor-associated antigens restrict the homogeneous accessibility of specific antibodies (*2,6*). Furthermore, tumor vascular architecture is highly unorthodox and may be comprised of variably perfused areas (*4,7*). Necrotic areas in the tumor mass have sparse vasculature, making them relatively avascular (*4*). Ultrastructural breaches in the vascular mural integrity (*8*) coupled with more hydrophilic and enlarged interstitium, should theoretically, be more conducive to extravasation and diffusion of the macromolecules (*5*). Yet the exaggerated interstitial pressures resulting from the compression of the ever-

Received Feb. 13, 1990; revision accepted Feb. 13, 1990.
For reprints contact: Jagat Narula, MD, Radiology Dept., Fifth Floor, Massachusetts General Hospital-East, Bldg. 149, 13th St., Charlestown, MA 02129.